# Spontaneous Organization of Supramolecular Rod-Bundles into a Body-Centered Tetragonal Assembly in Coil−Rod−Coil Molecules

**Myongsoo Lee,*,† Byoung-Ki Cho,† Yang-Gyu Jang,‡ and Wang-Cheol Zin‡**

*Contribution from the Department of Chemistry, Yonsei University, Shinchon 134, Seoul 120-749, Korea, and Department of Materials Science and Engineering, Pohang University of Science and Technology, Pohang 790-784, Korea*

*Received March 17, 2000*

**Abstract:** The synthesis and characterization of coil−rod−coil molecules of 4,4′-bis[4-methyloxypoly-(propyleneoxy)propyloxy-4′-biphenyloxymethyl]biphenyl with a poly(propylene oxide) coil of 3 (**7**), 6 (**8**), 9 (**9**), 13 (**10**), 17 (**11**), and 22 (**12**) propylene oxide units are described. These molecules self-assemble into ordered structures that differ significantly on variation of the length of poly(propylene oxide) coil. Coil−rod−coil molecule **7** self-organizes into lamellar crystalline and bicontinuous cubic liquid crystalline assemblies, while **8** shows a hexagonal columnar liquid crystalline assembly. Remarkably, increasing the length of coil induces discrete supramolecular aggregates that self-assemble into a birefringent 3-D superlattice. The molecules **9** and **10** assemble into discrete supramolecular aggregates that spontaneously organize into a novel 3-D tetragonal lattice with a body-centered symmetry in the crystalline and melt states. Further increasing the length of coil as in the case of **11** and **12** induces only a body-centered tetragonal crystalline phase, while the liquid crystalline phase in these molecules is suppressed. X-ray diffraction experiments and density measurements showed that the aggregation of these molecules into a discrete supramolecular structure gives rise to aromatic rod bundles with hockey puck-like cylindrical shape encapsulated by phase-separated coil segments which results in the formation of oblate aggregates. This nonspherical oblate shape is believed to be responsible for the formation of a body-centered tetragonal phase. These results demonstrate that supramolecular structures, from 1-D lamellar to 3-D tetragonal superlattices, formed by the self-assembling process of molecular rods can be controlled in a systematic and predictive way by simple variation of the length of grafted coils.

## Introduction

The development of new materials based on self-organizing systems has received a great deal of attention due to their potential in the construction of well-defined supramolecular nanostructures.[1−5] Especially, the construction of novel supramolecular architectures with well-defined shape and size by using rod building blocks is one of the most important subjects in organic material chemistry because they can exhibit novel electronic and photonic properties as a result of both their discrete dimensions and three-dimensional organization.[6]

Rod−coil systems consisting of rigid-rod and flexible coil segments are excellent candidates for creating well-defined supramolecular structures via a process of spontaneous organization.[2,7,8] The rod−coil molecular architecture imparts microphase separation of the rod and coil blocks into ordered periodic structures in nanoscale dimensions due to the mutual repulsion of the dissimilar blocks and the packing constraints imposed by the connectivity of each block, while the anisometric molecular shape and stiff rodlike conformation of the rod segment impart orientational organization. To balance these competing parameters, rod-coil molecules self-organize into a variety of supramolecular structures which can be controlled by variation of the rod-to-coil volume fraction.

Recently, we reported on the rod−coil diblock molecules containing poly(propylene oxide) as a coil segment.[9] These rod−coil molecules self-assemble into layered smectic, bicontinuous cubic, and hexagonal columnar liquid crystalline superlattices as the coil segment of the molecule increases in length relative to the rod segment. In a preliminary communication,[10] we demonstrated that introduction of the hydrophobic docosyl chain into the rod−coil diblock molecule containing the hydrophilic poly(ethylene oxide) coil gives rise to the formation of a spherical micellar phase with a lack of cubic symmetry. In

* To whom all correspondence should be addressed.
† Yonsei University.
‡ Pohang University of Science and Technology.

(1) Lehn, J. M. *Supramolecular Chemistry*; VCH: Weinheim, Germany, 1995.
(2) (a) Muthukumar, M.; Ober, C. K.; Thomas, E. L. *Science* **1997**, *277*, 1225. (b) Chen, J. T.; Thomas, E. L.; Ober, C. K.; Mao, G. *Science* **1996**, *273*, 343.
(3) Ruokolainen, J.; Makinen, R.; Yorkkeli, M.; Makela, T.; Serimaa, R.; ten Brinke, G.; Ikkala, O. *Science* **1998**, *280*, 557.
(4) Whitesides, G. M.; Mathias, J. P.; Seto, C. T. *Science* **1991**, *254*, 1312.
(5) Foester, S.; Antonietti, M. *Adv. Mater.* **1998**, *10*, 195.
(6) (a) Jenekhe, S. A.; Chen, X. L. *Science* **1998**, *279*, 1903. (b) Jenekhe, S. A.; Chen, X. L. *Science* **1999**, *283*, 372.
(7) (a) Williams, D. R. M.; Fredrickson, G. H. *Macromolecules* **1992**, *25*, 3561. (b) Raphael, E.; de Gennes, P. G. *Makromol. Chem., Macromol. Symp.* **1992**, *62*, 1.
(8) (a) Radzilowski, L. H.; Carragher, B. O.; Stupp, S. I. *Macromolecules* **1997**, *30*, 2110. (b) Stupp, S. I.; LeBonheur, V.; Walker, K.; Li, L. S.; Huggins, K. E.; Kesser, M.; Amstutz, A. *Science* **1997**, *276*, 384. (c) Tew, G. N.; Li, L.; Stupp, S. I. *J. Am. Chem. Soc.* **1998**, *120*, 5601. (d) Tew, G. N.; Pralle, M. U.; Stupp, S. I. *J. Am. Chem. Soc.* **1999**, *121*, 9825.
(9) (a) Lee, M.; Cho, B.-K.; Kim, H.; Yoon, J.-Y.; Zin, W.-C. *J. Am. Chem. Soc.* **1998**, *120*, 9168. (b) Lee, M.; Cho, B.-K.; Kim, H.; Zin, W.-C. *Angew. Chem., Int. Ed. Engl.* **1998**, *37*, 638. (c) Lee, M.; Oh, N.-K.; Zin, W.-C. *Chem. Commun.* **1996**, 1787. (d) Lee, M.; Cho, B.-K. *Chem. Mater.* **1998**, *10*, 1894.
(10) Lee, M.; Lee, D.-W.; Cho, B.-K.; Yoon, J.-Y.; Zin, W.-C. *J. Am. Chem. Soc.* **1998**, *120*, 13258.

10.1021/ja000966a CCC: $19.00 
Published on Web 07/25/2000

**Table 1.** Thermal Transitions of the Coil−Rod-Coil Molecules (data from second heating and first cooling scans)[a]

| molecule | $\bar{M}_w/\bar{M}_n$[b] | $f_{coil}$[c] | phase transitions (°C) and corresponding enthalpy changes (kJ/mol) | |
|---|---|---|---|---|
| | | | heating | cooling |
| **7** | 1.04 | 0.47 | k 160.2 (8.9), cub 231.2 (6.5), i | i 221.8 (4.2), cub 140.9 (10.6), k |
| **8** | 1.04 | 0.63 | k 91.8 (8.8), col 152.6 (2.3), i | i 149.7 (2.1), col 68.8 (6.2), k |
| **9** | 1.04 | 0.71 | k 81.0 (3.5), $M_{tet}$ 139.0 (3.4), i | i 132.8 (3.2), $M_{tet}$ 73.8 (3.5), k |
| **10** | 1.04 | 0.78 | k 84.5 (3.7), $M_{tet}$ 105.9 (2.4), i | i 98.3 (2.4), $M_{tet}$ 79.1 (3.7), k |
| **11** | 1.04 | 0.82 | k 79.3 (7.7), i | i 70.7 (7.2), k |
| **12** | 1.07 | 0.85 | k 56.2 (6.4), i | i 49.2 (5.2), k |

[a] k = crystalline, cub = bicontinuous cubic, col = hexagonal columnar, $M_{tet}$ = body-centered tetragonal micelle, i = isotropic. [b] Determined from GPC data. [c] $f_{coil}$ = coil volume fraction.

**Scheme 1.** Synthesis of Coil−Rod−Coil Molecules **7**−**12**

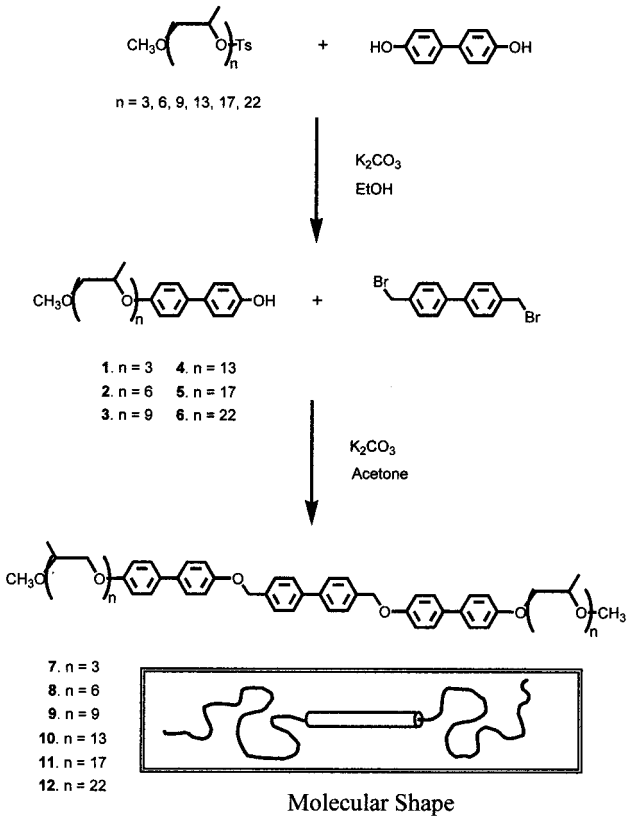


addition, we showed that the rod−coil approach as a means to manipulate supramolecular structure could be extended to main chain rod−coil multicblock copolymer systems which generate bicontinuous cubic and hexagonal columnar phases depending on the coil-to-rod volume fraction.[11] Our results on rod−coil systems imply that creation of novel supramolecular structures with regular shape and size is possible by using the self-organization process of stiff rod building blocks with covalently grafted flexible coils that in melt adopt coillike conformation. Accordingly, we have synthesized coil−rod−coil molecules to investigate the ability of rod building blocks to self-assemble into a discrete supramolecular bundle which can produce a 3-D organization.

We report here on the synthesis of coil−rod−coil triblock molecules containing poly(propylene oxide) (PPO) as coil blocks and their self-organization behavior characterized by optical polarized microscopy, differential scanning calorimetry (DSC), and X-ray diffraction measurements. These molecules depending on the coil length self-assemble into discrete supramolecular

(11) (a) Lee, M.; Cho, B.-K.; Kang, Y.-S.; Zin, W.-C. *Macromolecules* **1999**, *32*, 7688. (b) Lee, M.; Cho, B.-K.; Kang, Y.-S.; Zin, W.-C. *Macromolecules* **1999**, *32*, 8531.

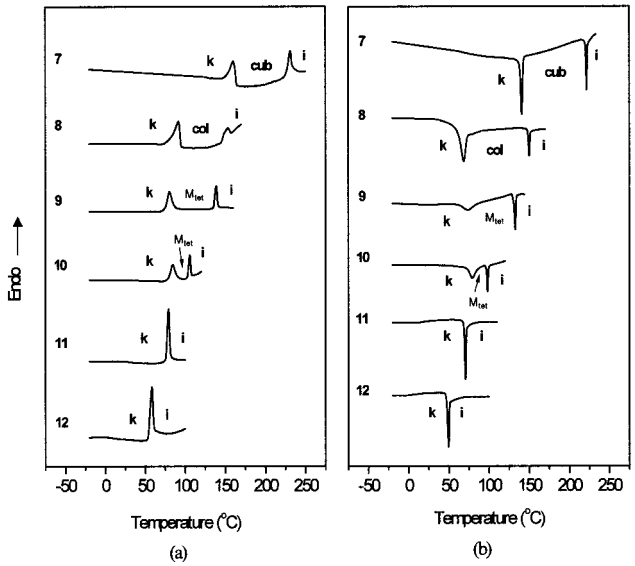


**Figure 1.** DSC traces exhibited during (a) the second heating scan and (b) the first cooling scan by **7**−**12**.

nanostructures which generate a novel body-centered tetragonal phase in their crystalline and melt states.

## Results and Discussion

**Synthesis and Thermal Characterization.** The synthesis of coil−rod−coil triblock molecules with different poly(propylene oxide) coil lengths was performed as outlined in Scheme 1. Monobiphenol terminated poly(propylene oxide)s **1**−**6** were prepared from the reaction of the appropriate monotosylated poly(propylene oxide) with an excess amount of 4,4′-biphenol. The coil−rod−coil triblock molecules **7**−**12** were obtained by treating corresponding precursor molecules **1**−**6** with 4,4′-bis-(bromomethyl)biphenyl in acetone in the presence of potassium carbonate. The resulting coil−rod−coil molecules were purified by column chromatography (silica gel) using ethyl acetate as an eluent until the polydispersity values remained constant. All analytical data of coil−rod−coil triblock molecules were consistent with expected molecular structures. Molecular weight distributions of these molecules determined from GPC appeared to be less than 1.07 as shown in Table 1, indicative of high purity. As confirmed by $^1$H NMR spectroscopy, the number of repeating units in poly(propylene oxide) coils of each triblock molecule determined from the ratio of the aromatic protons (ortho to alkoxy) to the ethylene protons of poly(propylene oxide) was in good agreement with the expected value.

The thermotropic phase behavior of the coil−rod−coil triblock molecules was studied using thermal optical polarized microscopy, DSC, and X-ray diffraction. Figure 1 presents the DSC heating and cooling traces of **7**−**12**, and the transition temperatures and the corresponding enthalpy changes deter-

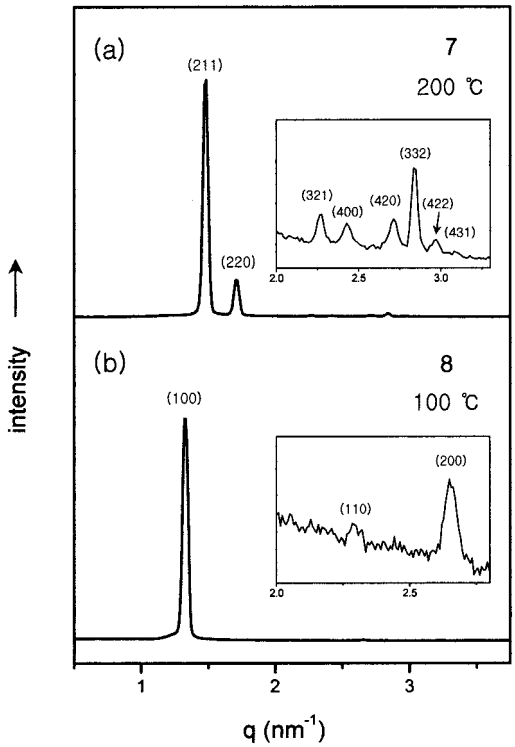


**Figure 2.** Representative SAXS spectra plotted against $q$ ($=4\pi \sin(\theta/\lambda)$) in (a) the bicontinuous cubic mesophase at 200 °C for **7** and (b) the hexagonal columnar mesophase at 100 °C for **8**.

mined from DSC scans are summarized in Table 1. As can be observed from Figure 1 and Table 1, coil−rod−coil molecule **7** exhibits a crystalline phase which melts into an optically isotropic cubic mesophase on heating. The X-ray diffraction pattern of **7** in the crystalline state displays three sharp reflections in the spacing ratio of 1:2:3 in the small-angle region, while two sharp reflections are observed in the wide-angle region, indicative of a lamellar structure consisting of microphase-separated crystalline rod domains and the amorphous coil domains.[12] The layer spacing of 38.3 Å corresponds to a rod tilt with the angle of 49° relative to the layer normal, considering the extended molecular length of 58 Å. In the melt state, the small-angle diffraction pattern shows a number of sharp reflections as shown in Figure 2a. The relative positions of these reflections are $\sqrt{6}$, $\sqrt{8}$, $\sqrt{14}$, $\sqrt{16}$, $\sqrt{20}$, $\sqrt{22}$, $\sqrt{24}$, and $\sqrt{26}$ which can be indexed as the 211, 220, 321 400, 420, 332, 422, and 431 reflections of a cubic phase with *Ia*3*d* symmetry with a lattice constant of 103.6 Å.[13] At a wide angle, only a diffuse halo remains as evidence of the lack of any positional long-range order other than the three-dimensional cubic packing of supramolecular units. On the basis of the X-ray diffraction result and its position in the phase sequence, located between lamellar crystalline and columnar liquid crystalline phases, the cubic phase can be considered as a bicontinuous cubic phase with *Ia*3*d* symmetry.[9] Assuming that a bicontinuous unit cell with *Ia*3*d* symmetry consists of a 3-D periodic minimal surface dividing the space similar to coil−coil block systems,[14] rod segments may be forming two interpenetrating trifunctional cylinder networks surrounded by coil segments. The resulting

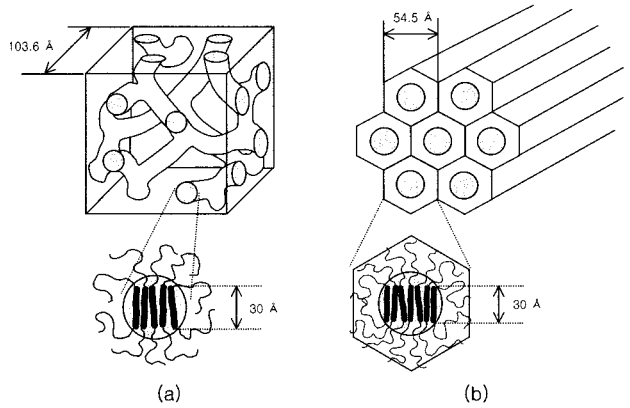


**Figure 3.** Schematic representation of (a) the self-assembly of **7** into the bicontinuous cubic phase and (b) the self-assembly of **8** into the hexagonal columnar phase.

aromatic networks are continuous through the space with 3-D periodicity as shown in Figure 3a.

In contrast to **7**, coil−rod−coil molecule **8** displays a birefringent mesophase upon crystalline melting. On cooling from the isotropic liquid of **8**, the formation of pseudo-focal conic domains can be observed, indicating the presence of a hexagonal columnar mesophase.[9,15] The X-ray diffraction patterns of the liquid crystalline phase of **8** display three sharp reflections with the ratio of 1:$\sqrt{3}$:2 in the small-angle region (Figure 2b), characteristic of the two-dimensional hexagonal structure. At wide angle only a diffuse halo remains, indicating that there are only liquidlike arrangements of rod segments within the columns. These results together with optical microscopic observations indicate that **8** displays a disordered hexagonal columnar mesophase with the lattice constant of 54.5 Å. Considering the lattice constant and measured density, the inner core of the column consists of rigid rods with an approximately square cross section as a result of parallel arrangements of rod units with their long axis, while the outer part consists of flexible coils which splay to fill the intercolumnar matrix (Figure 3b), similar to the results reported previously.[9a] The tendency to produce a columnar phase from a bicontinuous cubic phase on increasing the coil volume fraction is consistent with the results observed in our laboratory.[9−11] Our previous works showed that rod−coil molecules could self-assemble into a bicontinuous cubic phase as well as a hexagonal columnar phase simply by varying the rod versus coil volume fraction.

Remarkably, coil−rod−coil molecules **9** and **10** exhibit an unusual birefringent mesophase. On slow cooling from the isotropic liquid state of **9** and **10**, the formation of fern-like domains with rectangular shape growing in four directions which merge into a mosaic texture with straight edges could be observed on the polarized optical microscope, suggestive of the presence of a tetragonal order.[16] Taking into account the phase sequence existing at a larger coil volume fraction compared to that exhibiting a hexagonal columnar phase (Table 1), in analogy with lyotropic systems of amphiphilic molecules,[17] this bire-

(12) Lee, M.; Oh, N.-K.; Lee, H.-K.; Zin, W.-C. *Macromolecules* **1996**, *29*, 5567.

(13) Luzzati, V.; Spegt, P. A. *Nature* **1967**, *215*, 701. (b) Rancon, Y.; Charvolin, J. *J. Phys. Chem.* **1988**, *92*, 2646.

(14) Hajduk, D. A.; Harper, P. E.; Gruner, S. M.; Honeker, C. C.; Kim, G.; Thomas, E. L.; Fetters, L. J. *Macromolecules* **1994**, *27*, 4063.

(15) Destrade, C.; Foucher, P.; Gasparoux, H.; Nguyen, H. T. *Mol. Cryst. Liq. Cryst.* **1984**, *106*, 121.

(16) (a) Trzaska,. S. T.; Zheng, H.; Swager, T. M. *Chem. Mater.* **1999**, *11*, 130. (b) Ohta, K.; Higashi, R.; Ikejima, M.; Yamamoto, I.; Kobayashi, N. *J. Mater. Chem.* **1998**, *8*, 1979.

(17) (a) Mitchell, D. J.; Tiddy, G.; Warning, L.; Bostock, T.; McDonald, M. P. *J. Chem. Soc., Faraday Trans. 1* **1983**, *79*, 975. (b) Charvolin, J. *J. Chim. Phys.-Chim. Biol.* **1983**, *80*, 15. (c) Seddon, J. M. *Biochim. Biophys. Acta* **1990**, *1031*, 1. (d) Alexandridis, P.; Zhou, D.; Khan, A. *Langmuir* **1996**, *12*, 2690.

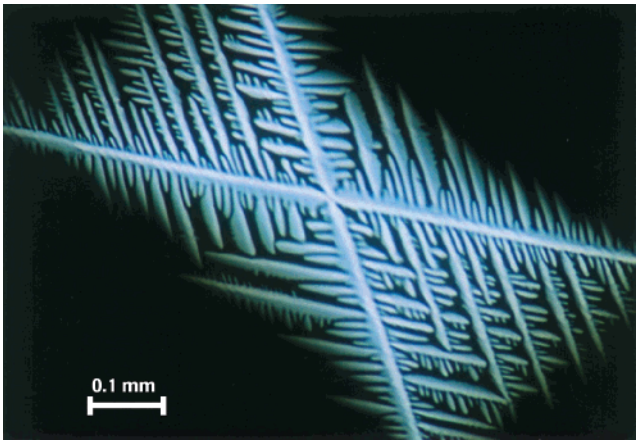


**Figure 4.** Representative optical polarized micrograph (100×) of the texture exhibited by the body-centered tetragonal micellar mesophase of **9** at the transition from the isotropic liquid state at 131 °C.

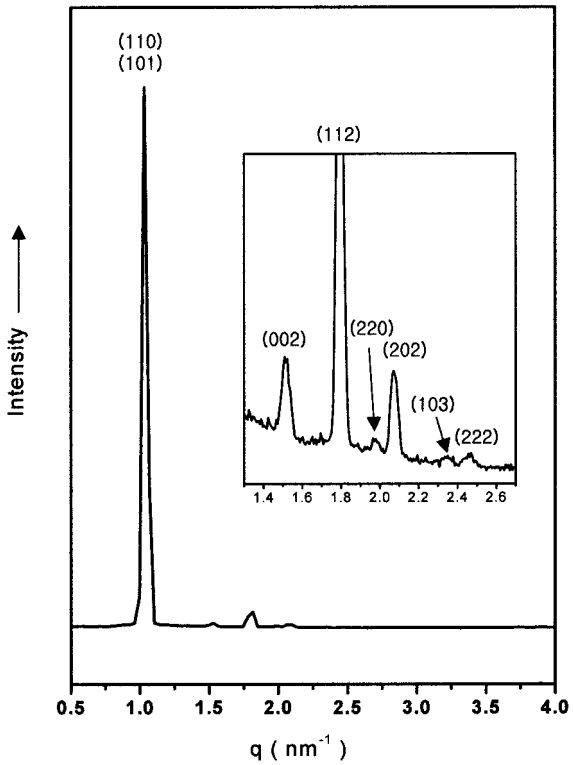


**Figure 5.** Small-angle X-ray diffraction pattern of **11** measured at 25 °C.

fringent mesophase may be considered as a discrete micellar phase. Figure 4 shows a representative texture exhibited by the birefringent micellar liquid crystalline phase of **9**. Further increasing the length of flexible coils as in the case of **11** and **12** suppresses the formation of liquid crystallinity.

**X-ray Diffraction Studies of 9−12.** To investigate the detailed supramolecular structure of **9**−**12**, X-ray scattering experiments were performed in the solid and melt states. In the solid state, all of these triblock molecules showed similar diffraction patterns with an identical spacing ratio. As shown in Figure 5, the small-angle X-ray diffraction patterns of these molecules show a sharp, low-angle high-intensity reflection and a number of sharp reflections of low intensity at higher angles. The observed reflections can be indexed as (110), (101), (002), (112), (220), (202), (103), and (222) planes of a three-dimensional tetragonal lattice with a body-centered unit cell (space group *I*4/*mmm*) with $c/a = 0.92$.[18] The wide-angle X-ray

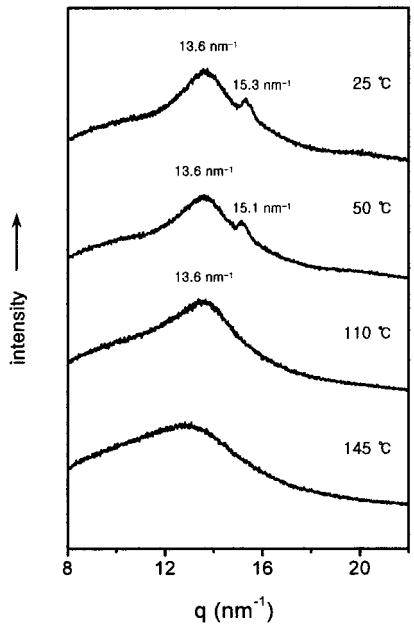


**Figure 6.** Wide-angle X-ray diffraction patterns of **9** measured at various temperatures.

**Table 2.** Small-Angle X-ray Diffraction Data for the Body-Centered Tetragonal Structure of **11**[a]

| *h* | *k* | *l* | $q_{calcd}$ nm$^{-1}$ | $q_{obsd}$ nm$^{-1}$ | *h* | *k* | *l* | $q_{calcd}$ nm$^{-1}$ | $q_{obsd}$ nm$^{-1}$ |
|---|---|---|---|---|---|---|---|---|---|
| 1 | 1 | 0 | 0.991 | 0.991 | 2 | 2 | 0 | 1.971 | 1.979 |
| 1 | 0 | 1 | 1.032 | 1.032 | 2 | 0 | 2 | 2.064 | 2.072 |
| 2 | 0 | 0 | 1.393 | | 3 | 1 | 0 | 2.208 | |
| 0 | 0 | 2 | 1.517 | 1.517 | 3 | 0 | 1 | 2.218 | |
| 2 | 1 | 1 | 1.733 | | 1 | 0 | 3 | 2.383 | 2.356 |
| 1 | 1 | 2 | 1.806 | 1.796 | 2 | 2 | 2 | 2.487 | 2.463 |

[a] $q_{obsd}$ and $q_{calcd}$ are the scattering vectors of the observed reflections (Figure 5) and calculated for the body-centered tetragonal structure with lattice parameters $a = 8.99$ nm and $c = 8.27$ nm ($c/a = 0.92$).

diffraction patterns show two reflections at *q*-spacings of 13.6 and 15.3 nm$^{-1}$, which are presumably due to crystal packing of rod segments within aromatic domains (Figure 6).

It should be noted that the observed SAXS reflections agree well with the expected relative peak positions for a body-centered tetragonal structure with $c/a = 0.92$ (Table 2). The observed *d* spacings and the lattice constants *a* and *c* are summarized in Table 3. Interestingly, the rate of increase in *a* and *c* with increasing the number of propylene oxide units remains constant as shown in Table 3. The similar diffraction patterns have been observed in the intermediate phase called the "T phase" between lamellar and columnar phases of surfactant molecules, which represents a tetragonally perforated lamellar structure.[18,19] In contrast to that of surfactant molecules, the tetragonal phase of the coil−rod−coil molecules occurs on increase in the coil volume fraction, compared to that of **8** which show a hexagonal columnar phase. Therefore, it can be concluded that this phase represents a tetragonal phase consisting of a 3-D body-centered arrangement of discrete supramolecular aggregates as discussed earlier.

The indexing of the diffraction data to a discrete micellar tetragonal structure can also be accessed by plotting the aggregate volume ($a^2c/2$) as a function of molar volume ($V_m$) of coil−rod−coil molecules. For discrete supramolecular aggregates, such a plot should be linear and the extrapolation should pass through the origin. As shown in Figure 7, the

(18) Luzzati, V.; Tardieu, A.; Gulik-Krzwicki, T. *Nature* **1968**, *217*, 1028.
(19) Kekicheff, P.; Tiddy, G. J. T. *J. Phys. Chem.* **1989**, *93*, 2520.

**Table 3.** Characterization of Coil−Rod−Coil Molecules **9**−**12** by Small-Angle X-ray Scattering

| | crystalline phase | | | | | | | | liquid crystalline phase | | | |
|---|---|---|---|---|---|---|---|---|---|---|---|---|
| | | | | | body-centered tetragonal | | | | body-centered tetragonal | | | |
| | density (g/cm$^3$) | | | | | | lattice constant | | | | lattice constant | |
| molecule | [a]$\rho$ | [b]$\rho_{rod}$ | $n$[c] | $d$ (Å)[d] | $d_{101}$ (Å) | $d_{002}$ (Å) | $a$ (Å) | $c$ (Å) | $d_{101}$ (Å) | $d_{002}$ (Å) | $a$ (Å) | $c$ (Å) |
| **9** | 1.070 | 1.240 | 87 | 52 | 52.9 | 35.9 | 78.3 | 71.9 | 48.8 | 35.3 | 76.7 | 70.6 |
| **10** | 1.055 | 1.247 | 81 | 50 | 56.8 | 38.2 | 83.2 | 76.5 | 56.9 | 39.0 | 84.0 | 78.0 |
| **11** | 1.044 | 1.244 | 82 | 50 | 60.9 | 41.4 | 89.9 | 82.7 | | | | |
| **12** | 1.034 | 1.231 | 87 | 52 | 66.8 | 45.4 | 98.7 | 90.8 | | | | |

[a] $\rho$ = molecular density. [b] $\rho_{rod}$ = density of rod segment. [c] Number of molecules in a micelle. [d] Diameter of rod bundles.

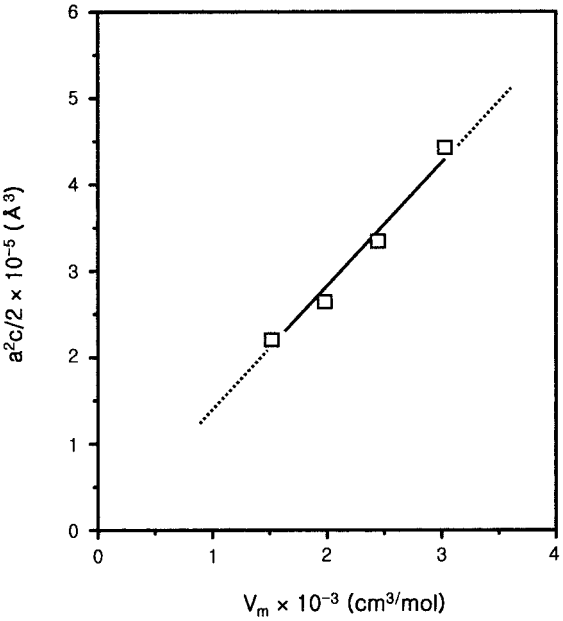


**Figure 7.** The dependence of the volume of a micelle ($a^2c/2$) on the molar volume ($V_m$) of **9**−**12**.

variation in the volume of a micelle shows a linear dependence as a function of the molar volume ($V_m$), and the extrapolation to $a^2c/2 = 0$ gives zero molecular volume. To describe the detailed supramolecular structure, it is desirable to calculate the number of molecules per micelle. From the lattice constants and the densities, the average number ($n$) of molecules can be estimated according to eq 1, where $M$ is the molecular weight, $\rho$ is molecular density, and $N_A$ is Avogadro's number.

$$n = a^2 c \frac{N_A \rho}{2M} \quad (1)$$

As shown in Table 3, **9**, **10**, **11**, and **12** are calculated to have approximately 84 molecules in each micelle, which indicates the similar number of molecules per micelle irrespective of the variation in the number of propylene oxide units. From the rod densities ($\rho_{rod}$) (Table 3) and the molecular weight of the rod segment ($M_{rod}$), the diameter ($d = 2r$) of the aromatic core can be calculated according to eq 2, where $r$ is radius of the aromatic core and $h$ is the length of the rod segment. The

$$\pi r^2 h = \frac{n M_{rod}}{N_A \rho_{rod}} \quad (2)$$

aggregation of approximately 84 rod segments in a micelle can be estimated to give rise to a supramolecular rod bundle with a hockey puck-like cylinder shape 50 Å in diameter and 30 Å in length (estimated from CPK models), considering that the rods are aligned axially with their preferred direction in the crystalline state.

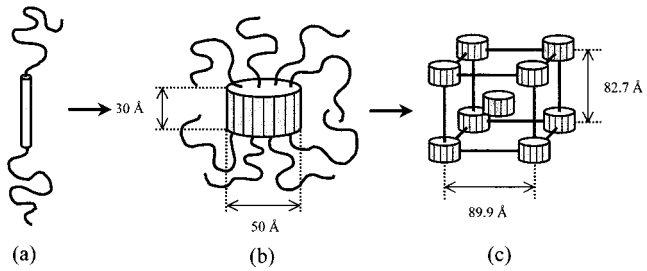


**Figure 8.** Schematic representation of the self-assembly of (a) coil−rod−coil molecules **11** into (b) a supramolecular bundle and the subsequent formation of (c) the body-centered tetragonal superlattice.

On the basis of the X-ray results and the above calculations, schematic representations can be constructed as shown in Figure 8. The inner core of the supramolecular structure is constituted by the discrete rod bundle that is encapsulated with phase-separated poly(propylene oxide) coils, which give rise to the formation of the nonspherical oblate aggregate. The suprmolecular rod bundles self-organize into a 3-D body-centered tetragonal symmetry. The oblate shape of supramolecular aggregates is believed to be responsible for the formation of the unusual 3-D tetragonal phase. This estimation is further supported by the fact that a tetragonal lattice constant ($c$) obtained from SAXS is in reasonable agreement with the length of the rod−coil molecule assuming curling of the coils and optical textures appear to be birefringent.

Small-angle X-ray diffraction studies of the birefringent liquid crystalline phase of **9** and **10** show similar diffraction patterns to those of their solid state, indicating the presence of a three-dimensional tetragonal order with a body-centered symmetry. The observed $d$ spacings, lattice constants, and calculated number of molecules in each micelle are shown in Table 3. At the wide-angle region, only a diffuse halo remains as shown in Figure 6. These results together with optical microscopic observations indicate that **9** and **10** display a body-centered tetragonal micellar liquid crystalline phase.

The self-organization of rod segments into discrete bundles with hockey puck-like cylindrical core shape is well illustrated by the rod−coil theories that relates the volume fraction of rod and shape of aggregation.[7a,20] Our discrete supramolecular structures are formed by molecular structures that differ only in the number of repeating units of coil segments and hence in the volume fraction of coil segments relative to rod segments, compared to that exhibiting a hexagonal columnar phase. Columnar ordering of rod segments would confine rod−coil junctions to a 2-D interface with a relatively high density of grafting site, which forces a strong stretching of the coils away from the interface, and thus the system is energetically unfavor-

(20) Halperin, A. *Macromolecules* **1990**, *23*, 2724.

able. Consequently, the columnar rod-domains will break into regular fragments consisting of rod bundles by three dimensionally splaying the coil segments, to maximize the entropy of the grafted coils and fill space efficiently.

In most cases for thermotropic,[21] lyotropic,[17,22] and coil−coil block copolymer systems,[23] discrete micelles organize into different cubic phases (mainly primitive, body centered, and face centered) which are all optically isotropic. Although the existence of a tetragonal structure has been observed in block copolymers consisting of polystyrene and side chain liquid crystalline polymer, it appeared to be 2-dimensional.[24] Thus, a notable feature of our system is the ability of the molecular rods to self-assemble into discrete supramolecular bundles that generate a 3-D tetragonal superlattice in the solid and melt states. This unique phase behavior probably originated from the anisotropic aggregation of rod segments with their long axes within microphase separated aromatic domains. Consequently, rod bundles with puck-like cylindrical shape would give rise to oblate micelles which can pack more densely into an optically anisotropic 3-dimensional tetragonal lattice, rather than an optically isotropic cubic lattice. These results demonstrate that discrete supramolecular rod bundles encapsulated by flexible coils can be created by introducing appropriate poly(propylene oxide) coils to each end of a molecular rod.

## Conclusion

The coil−rod−coil molecules based on poly(propylene oxide) as coils were synthesized and their self-assembling behavior in solid and melt states was investigated. These molecules were observed to organize into ordered structures that differ significantly on increasing the length of the coil. The coil−rod−coil molecule with a short length of coils (**7**) self-organizes into lamellar crystalline and bicontinuous cubic liquid crystalline assemblies, while the coil−rod−coil molecule with medium length of coils (**8**) shows a 2-D hexagonal columnar liquid crystalline assembly. Remarkably, the molecules with longer length coils (**9** and **10**) assemble into discrete supramolecular aggregates that spontaneously organize into a novel 3-D tetragonal phase with a body-centered symmetry in the solid and melt states. Further increasing the length of coils as in the case of **11** and **12** gives rise to only a body-centered tetragonal crystalline phase. Calculations based on the lattice constants of 3-D tetragonal symmetry and densities have shown that the organization of the triblock molecules into a supramolecular structure can give rise to an aromatic core with puck-like cylindrical shape which is a cause of the formation of oblate aggregates. This nonspherical oblate shape of the supramolecular aggregates seems to be responsible for the formation of a body-centered tetragonal lattice. This result suggests that our approach of controlling supramolecular structures using rod building blocks by only a small variation in the length of grafted coils allows novel highly ordered 3-D nanostructures to be produced.

## Experimental Section

**Materials.** 4,4′-Biphenol (99%), toluene-*p*-sulfonyl chloride (98%), and 4,4′-bis(bromomethyl)biphenyl (99%) from Tokyo Kasei were used as received. Poly(propylene glycol)s of ({DP}) 3, 6, 13, 17, and 22 (all from Aldrich) and the other conventional reagents were used as received. Poly(propylene glycol) of ({DP}) 9 was synthesized according to the procedure described previously.[9]

**Techniques.** $^1$H NMR spectra were recorded from $CDCl_3$ solutions on a Bruker AM 250 spectrometer. The purity of the products was checked by thin-layer chromatography (TLC; Merck, silica gel 60). A Perkin-Elmer DSC-7 differential scanning calorimeter equipped with a 1020 thermal analysis controller was used to determine the thermal transitions, which were reported as the maxima and minima of their endothermic or exothermic peaks. In all cases, the heating and cooling rates were 10 °C min$^{-1}$. A Nikon Optiphot 2-pol optical polarized microscope (magnification: 100×) equipped with a Mettler FP 82 hot-stage and a Mettler FP 90 central processor was used to observe the thermal transitions and to analyze the anisotropic texture. Microanalyses were performed with a Perkin-Elmer 240 elemental analyzer at the Organic Chemistry Research Center. X-ray scattering measurements were performed in transmission mode with synchrotron radiation at the 3C2 X-ray beam line at the Pohang Accelerator Laboratory, Korea. To investigate structural changes on heating, the sample was held in an aluminum sample holder which was sealed with a window of 7 $\mu$m thick Kapton films on both sides. The sample was heated with two catridge heaters and the temperature of the samples was monitored by a thermocouple placed close to the sample. Background scattering correction was made by subtracting the scatterings from the Kapton. Molecular weight distributions ($\bar{M}_w/\bar{M}_n$) were determined by gel permeation chromatography (GPC) with a Waters R401 instrument equipped with Stragel HR 3, 4, and 4E columns, a M7725i manual injector, a column heating chamber, and a 2010 Millennium data station. Measurements were made by using a UV detector, with $CHCl_3$ as solvent (1.0 mL min$^{-1}$). The molecular density ($\rho$) measurements were performed in an aqueous sodium chloride solution at 25 °C. The densities of poly(propylene oxide) coils were used as $\rho_{PPO} = 1.0$ g/cm$^3$.[25] The rod densities ($\rho_{rod}$) of each molecule were calculated on the basis of $\rho$ and $\rho_{PPO}$.

**Synthesis.** A general outline of the synthetic procedure is shown in Scheme 1. **4-[Methyloxypoly(propyleneoxy)propyloxy]-4′-phenylphenol (1−6).** 4-[Methyloxypoly(propyleneoxy)propyloxy]-4′-phenylphenols (**1**−**6**) were synthesized using a similar procedure described previously.[11]

**1**: yield 77%; $^1$H NMR (250 MHz, $CDCl_3$, $\delta$, ppm) 7.36−7.42 (m, 4Ar-H, *m* to OH, *m* to $OCH_2CH$ or $OCH(CH_3)$), 6.86−6.95 (m, 4Ar-H, *o* to OH, *o* to $OCH_2CH$ or $OCH(CH_3)$), 4.54 (m, phenyl-$OCH_2CH(CH_3)$ or $CH_2CH(CH_3)O$-phenyl), 3.30−4.10 (m, $CH_3O$ and $OCH_2CH(CH_3)$), 1.00−1.55 (m, 9H, $CH(CH_3)O$); $\bar{M}_w/\bar{M}_n = 1.03$ (GPC).

**2**: yield 58%; $^1$H NMR (250 MHz, $CDCl_3$, $\delta$, ppm) 7.36−7.42 (m, 4Ar−H, *m* to OH, *m* to $OCH_2CH$ or $OCH(CH_3)$), 6.86−6.95 (m, 4Ar-H, *o* to OH, *o* to $OCH_2CH$ or $OCH(CH_3)$), 4.53 (m, phenyl-$OCH_2CH(CH_3)$ or $CH_2CH(CH_3)O$-phenyl), 3.30−3.85 (m, $CH_3O$ and $OCH_2CH(CH_3)$), 0.90−1.40 (m, 18H, $CH(CH_3)O$); $\bar{M}_w/\bar{M}_n = 1.04$ (GPC).

**3**: yield 63%; $^1$H NMR (250 MHz, $CDCl_3$, $\delta$, ppm) 7.36−7.42 (m, 4Ar-H, *m* to OH, *m* to $OCH_2CH$ or $OCH(CH_3)$), 6.86−6.95 (m, 4Ar-H, *o* to OH, *o* to $OCH_2CH$ or $OCH(CH_3)$), 4.52 (m, phenyl-$OCH_2CH(CH_3)$ or $CH_2CH(CH_3)O$-phenyl), 3.20−3.85 (m, $CH_3O$ and $OCH_2CH(CH_3)$), 0.90−1.45 (m, 27H, $CH(CH_3)O$); $\bar{M}_w/\bar{M}_n = 1.04$ (GPC).

**4**: yield 70%; $^1$H NMR (250 MHz, $CDCl_3$, $\delta$, ppm) 7.38−7.44 (m, 4Ar-H, *m* to OH, *m* to $OCH_2CH$ or $OCH(CH_3)$), 6.86−6.98 (m, 4Ar-H, *o* to OH, *o* to $OCH_2CH$ or $OCH(CH_3)$), 4.53 (m, phenyl-$OCH_2CH(CH_3)$ or $CH_2CH(CH_3)O$-phenyl), 3.20−3.85 (m, $CH_3O$ and $OCH_2CH(CH_3)$), 0.85−1.40 (m, 39H, $CH(CH_3)O$); $\bar{M}_w/\bar{M}_n = 1.04$ (GPC).

**5**: yield 65%; $^1$H NMR (250 MHz, $CDCl_3$, $\delta$, ppm) 7.38−7.44 (m, 4Ar-H, *m* to OH, *m* to $OCH_2CH$ or $OCH(CH_3)$), 6.86−6.97 (m, 4Ar-

(21) (a) Percec, V.; Cho, W.-D.; Mosier, P. E.; Ungar, G.; Yeardley, D. J. P. *J. Am. Chem. Soc.* **1998**, *120*, 11061. (b) Balagurusamy, V. S. K.; Ungar, G.; Percec, V.; Johansson, G. *J. Am. Chem. Soc.* **1997**, *119*, 1539. (c) Yeardley, D. J. P.; Ungar, G.; Percec, V.; Holerca, M. N.; Johansson, G. *J. Am. Chem. Soc*. **2000**, *122*, 1684. (d) Borisch, K.; Diele, S.; Goering, P.; Kresse, H.; Tschierske, C. *J. Mater. Chem.* **1998**, *8*, 529. (e) Borisch, K.; Diele, S.; Goering, P.; Mueller, H.; Tschierske, C. *Liq. Cryst.* **1997**, *22*, 427.

(22) (a) Fairhurst, C. E.; Fuller, S.; Gray, J.; Holmes, M. C.; Tiddy, G. J. T. *Handbook of Liquid Crystals*; Demus, D., Goodby, J., Gray, G. W., Spiess, H.-W., Vill, V., Eds.; Wiley-VCH: Weinheim, Germany, 1998; Vol. 3, Chapter 7. (b) Luzzati, V.; Vargas, R.; Gulik, A.; Mariani, P.; Seddon, J. M.; Rivas, E. *Biochemistry* **1992**, *31*, 279. (c) Gulik, A.; Delacroix, H.; Kirschner, G.; Luzzati, V. *J. Phys. II (France)* **1995**, *5*, 445.

(23) (a) Thomas, E. L.; Kinning, D. J.; Alward, D. B.; Henkee, C. S. *Macromolecules* **1987**, *20*, 2934. (b) Sakamoto, N.; Hashimoto, T. *Macromolecules* **1998**, *31*, 8493.

(24) Fischer, H. *Polymer* **1994**, *35*, 3786.

(25) Van Krevelen, D. W. *Property of Polymers*; Elsevier: New York, 1990.

H, *o* to OH, *o* to $OCH_2CH$ or $OCH(CH_3)$), 4.52 (m, phenyl-$OCH_2CH(CH_3)$ or $CH_2CH(CH_3)O$-phenyl), 3.18−3.90 (m, $CH_3O$ and $OCH_2CH(CH_3)$), 0.83−1.40 (m, 51H, $CH(CH_3)O$); $\bar{M}_w/\bar{M}_n$ = 1.05 (GPC).

**6**: yield 73%; $^1$H NMR (250 MHz, $CDCl_3$, $\delta$, ppm) 7.38−7.44 (m, 4Ar-H, *m* to OH, *m* to $OCH_2CH$ or $OCH(CH_3)$), 6.86−6.98 (m, 4Ar-H, *o* to OH, *o* to $OCH_2CH$ or $OCH(CH_3)$), 4.54 (m, phenyl-$OCH_2CH(CH_3)$ or $CH_2CH(CH_3)O$-phenyl), 3.20−3.90 (m, $CH_3O$ and $OCH_2CH(CH_3)$), 0.80−1.40 (m, 66H, $CH(CH_3)O$); $\bar{M}_w/\bar{M}_n$ = 1.07 (GPC).

**4,4′-Bis[4-methyloxypoly(propyleneoxy)propyloxy-4′-biphenyloxymethyl]biphenyls (7−12).** 4,4′-Bis[4-methyloxypoly(propyleneoxy)propyloxy-4′-biphenyloxymethyl]biphenyls **7**, **8**, **9**, **10**, **11**, and **12** were all synthesized using the same procedure. A representative example is described for **7**. 4-[Methyloxypoly(propyleneoxy)propyloxy]-4′-phenylphenol (**1**) (0.77 g, 2.07 mmol), 4,4′-bis(bromomethyl)biphenyl (0.32 g, 0.94 mmol), and excess $K_2CO_3$ were dissolved in 30 mL of acetone. The mixture was heated at reflux for 12 h and then cooled to room temperature. The solvent was removed in a rotary evaporator, and the resulting mixture was poured into water and extracted with methylene chloride. The methylene chloride solution was washed with water, dried over anhydrous magnesium sulfate, and filtered. After the solvent was removed in a rotary evaporator, the crude product was purified by column chromatography (silica gel, ethyl acetate eluent) to yield 0.47 g (54%) of a white solid. $^1$H NMR (250 MHz, $CDCl_3$, $\delta$, ppm) 7.44−7.65 (m, 16Ar-H, *m* to $OCH_2$phenyl, *m* to $OCH_2CH$ or $OCH(CH_3)$, *o* to $CH_2O$-phenyl and *m* to $CH_2O$-phenyl), 6.96−7.07 (m, 8Ar-H, *o* to $OCH_2$-phenyl, *o* to $OCH_2CH$ or $OCH(CH_3)$), 5.15 (s, 4H, $OCH_2$-phenyl), 4.55 (m, phenyl-$OCH_2CH(CH_3)$ or $CH_2CH(CH_3)O$-phenyl), 3.25−4.10 (m, $OCH_2CH(CH_3)$ and $OCH_3$), 0.90−1.55 (m, 18H, $CH(CH_3)O$); $\bar{M}_w/\bar{M}_n$ = 1.04 (GPC). Anal. Calcd for $C_{58}H_{78}O_{10}$: C, 74.49; H, 8.41. Found: C, 74.55; H, 8.02.

**8**: yield 57%; $^1$H NMR (250 MHz, $CDCl_3$, $\delta$, ppm) 7.44−7.65 (m, 16Ar-H, *m* to $OCH_2$-phenyl, *m* to $OCH_2CH$ or $OCH(CH_3)$, *o* to $CH_2$-Ophenyl and *m* to $CH_2O$-phenyl), 6.96−7.07 (m, 8Ar-H, *o* to $OCH_2$-phenyl, *o* to $OCH_2CH$ or $OCH(CH_3)$), 5.15 (s, 4H, $OCH_2$-phenyl), 4.53 (m, phenyl-$OCH_2CH(CH_3)$ or $CH_2CH(CH_3)O$-phenyl), 3.18−3.82 (m, $OCH_2CH(CH_3)$ and $OCH_3$), 0.85−1.55 (m, 36H, $CH(CH_3)O$); $\bar{M}_w/\bar{M}_n$ = 1.04 (GPC). Anal. Calcd for $C_{76}H_{114}O_{16}$: C, 71.11; H, 8.95. Found: C, 71.16; H, 8.93.

**9**: yield 61%; $^1$H NMR (250 MHz, $CDCl_3$, $\delta$, ppm) 7.44−7.65 (m, 16Ar-H, *m* to $OCH_2$-phenyl, *m* to $OCH_2CH$ or $OCH(CH_3)$, *o* to $CH_2O$-phenyl and *m* to $CH_2O$-phenyl), 6.96−7.06 (m, 8Ar−H, *o* to $OCH_2$-phenyl, *o* to $OCH_2CH$ or $OCH(CH_3)$), 5.14 (s, 4H, $OCH_2$-phenyl), 4.53 (m, phenyl-$OCH_2CH(CH_3)$ or $CH_2CH(CH_3)O$-phenyl), 3.16−3.90 (m, $OCH_2CH(CH_3)$ and $OCH_3$), 0.85−1.60 (m, 54H, $CH(CH_3)O$); $\bar{M}_w/\bar{M}_n$ = 1.04 (GPC). Anal. Calcd for $C_{94}H_{150}O_{22}$: C, 69.17; H, 9.26. Found: C, 69.18; H, 9.24.

**10**: yield 62%; $^1$H NMR (250 MHz, $CDCl_3$, $\delta$, ppm) 7.43−7.65 (m, 16Ar-H, *m* to $OCH_2$-phenyl, *m* to $OCH_2CH$ or $OCH(CH_3)$, *o* to $CH_2O$-phenyl and *m* to $CH_2O$-phenyl), 6.95−7.06 (m, 8Ar-H, *o* to $OCH_2$-phenyl, *o* to $OCH_2CH$ or $OCH(CH_3)$), 5.14 (s, 4H, $OCH_2$-phenyl), 4.53 (m, phenyl-$OCH_2CH(CH_3)$ or $CH_2CH(CH_3)O$-phenyl), 3.18−3.82 (m, $OCH_2CH(CH_3)$ and $OCH_3$), 0.85−1.58 (m, 78H, $CH(CH_3)O$); $\bar{M}_w/\bar{M}_n$ = 1.04 (GPC). Anal. Calcd for $C_{118}H_{190}O_{30}$: C, 67.85; H, 9.17. Found: C, 67.84; H, 9.19.

**11**: yield 67%; $^1$H NMR (250 MHz, $CDCl_3$, $\delta$, ppm) 7.43−7.65 (m, 16Ar-H, *m* to $OCH_2$-phenyl, *m* to $OCH_2CH$ or $OCH(CH_3)$, *o* to $CH_2O$-phenyl and *m* to $CH_2O$phenyl), 6.95−7.06 (m, 8Ar-H, *o* to $OCH_2$-phenyl, *o* to $OCH_2CH$ or $OCH(CH_3)$), 5.14 (s, 4H, $OCH_2$-phenyl), 4.53 (m, phenyl-$OCH_2CH(CH_3)$ or $CH_2CH(CH_3)O$-phenyl), 3.16−3.83 (m, $OCH_2CH(CH_3)$ and $OCH_3$), 0.82−1.58 (m, 102H, $CH(CH_3)O$); $\bar{M}_w/\bar{M}_n$ = 1.04 (GPC). Anal. Calcd for $C_{142}H_{238}O_{38}$: C, 66.80; H, 9.39. Found: C, 66.83; H, 9.46.

**12**: yield 55%; $^1$H NMR (250 MHz, $CDCl_3$, $\delta$, ppm) 7.43−7.65 (m, 16Ar-H, *m* to $OCH_2$-phenyl, *m* to $OCH_2CH$ or $OCH(CH_3)$, *o* to $CH_2O$-phenyl and *m* to $CH_2O$-phenyl), 6.95−7.06 (m, 8Ar-H, *o* to $OCH_2$-phenyl, *o* to $OCH_2CH$ or $OCH(CH_3)$), 5.14 (s, 4H, $OCH_2$-phenyl), 4.53 (m, phenyl-$OCH_2CH(CH_3)$ or $CH_2CH(CH_3)O$-phenyl), 3.12−3.90 (m, $OCH_2CH(CH_3)$ and $OCH_3$), 0.75−1.55 (m, 132H, $CH(CH_3)O$); $\bar{M}_w/\bar{M}_n$ = 1.07 (GPC). Anal. Calcd for $C_{172}H_{298}O_{48}$: C, 65.91; H, 9.58. Found: C, 66.08; H, 9.57.

**Acknowledgment.** Financial support of this work by the Korea Science and Engineering Foundation (1999-1-308-002-3), CRM-KOSEF (2000), the Brain Korea 21 Project, and the Synchrotron Radiation Source at Pohang, Korea (for the beam time and technical assistance) is gratefully acknowledged. W.-C. Zin acknowledges the Korea Research Foundation (1998-017-E00211) for financial support.

**Supporting Information Available:** A representative optical micrograph for **9**, WAXS curves of **7**, and SAXS patterns of **10** and **12** (PDF). This material is available free of charge via the Internet at http://pubs.acs.org.

JA000966A